European **J**ournal of **Chem**istry

Check for updates

Synthesis, characterization and thermal decomposition of ethyl-2'-amino-5'-cyano-6'-(1*H*-indole-3yl)-2-oxospiro[indoline-3,4'-pyran]-3'-carboxylate under non-isothermal condition in nitrogen atmosphere

Ganesan Nalini [ID] 1,*, Natesan Jayachandramani [ID] 2, Radhakrishnan Suresh [ID] 3,
Prakasam Thirumurugan [ID] 4, Venugopal Thanikachalam [ID] 5, Govindasamy Manikandan [ID] 5
and Dharmalingam Sankari [ID] 1

1 *Department of Biotechnology, Faculty of Science and Humanities, SRM Institute of Science and Technology, Kattankulathur, 603203, India*
nalini7680@gmail.com (G.N.), sankari.biotech09@gmail.com (D.S.)
2 *Department of Chemistry, Pachaiyappa's College, Chennai, 600030, India*
njmani53@gmail.com (N.J.)
3 *Department of Chemistry, Presidency College, Chennai, 600005, India*
sureshradhakrishnan7680@gmail.com (R.S.)
4 *Department of Chemistry, New York University, Abu Dhabi, United Arab Emirates*
ptm.org@gmail.com (P.T.)
5 *Department of Chemistry, Annamalai University, Annamalainagar, 608002, India*
profvt.chemau@gmail.com (V.T.), phdmani@gmail.com (G.M.)

* *Corresponding author at: Department of Biotechnology, Faculty of Science and Humanities, SRM Institute of Science and Technology, Kattankulathur, 603203, India.*
Tel: +91.44.27417777 Fax: +91.44.27453903 e-mail: nalini7680@gmail.com (G.Nalini).

RESEARCH ARTICLE

ABSTRACT

A new compound, spiro-oxindole derivative compound namely ethyl-2'-amino-5'-cyano-6'-(1*H*-indole-3yl)-2-oxospiro[indoline-3,4'-pyran]-3'-carboxylate (EACIOIPC) has been synthesized and characterized by microanalysis, FT-IR, mass spectrum and NMR (^{1}H and ^{13}C) techniques. The thermal decomposition of the compound was studied by thermogravimetric analysis under dynamic nitrogen atmosphere at different heating rates of 10, 15, 20 and 30 K/min. The kinetic parameters were calculated using model-free (Friedman's, Kissinger-Akahira-Sunose (KAS) and Flynn-Wall-Ozawa (FWO) methods) and model-fitting (Coats and Redfern (CR)) methods. The decomposition process of EACIOIPC followed a single step mechanism as evidenced from the data. Existence of compensation effect is noticed for the decomposition of EACIOIPC. Invariant kinetic parameters are consistent with the average values obtained by Friedman and KAS in conversional methods.

Cite this: *Eur. J. Chem.* **2019**, *10(1)*, 72-81 | **Journal website**: www.eurjchem.com

1. Introduction

The spiro-oxindole framework is an important structural organization and the core structure of a variety of medicinal agents and natural products [1,2]. The spiro-oxindole derivatives have been described with different biological activities, such as anti-tumor [3], anti-inflammatory, analgesic, antimicrobial, anti-HIV, antimalarial activity and as antipyretic agents [4]. Compounds such as of 5-[(indol-2-on-3-yl)methyl]-2,2-dimethyl-1,3-dioxane-4,6-diones and spiro-cyclopropylox-indole derivatives have been reported to behave as poliovirus and rhinovirus and potential aldose reductase inhibitors.

Spiro-pyrrolidinyloxindoles have been extensively studied as potent inhibitors of p53-MDM2 interaction, finally leading to the identification of MI-888, which could achieve rapid, complete and durable tumor regression in xenograft models of human cancer advanced preclinical research for cancer therapy [5]. Spiro-oxindole systems are of great interest in modern organic, medicinal, and natural product chemistry. This type of framework forms a core structure of many alkaloids with promising pharmacological activity, such as horsfiline, gelsemine, mitraphylline and spirotryprotatins A,B [6]. Novel di-spiro-oxindole-pyrrolidine derivatives have been synthesized through 1,3-dipolar cycloaddition of an azomet-

Figure 1. Structure of ethyl-2'-amino-5'-cyano-6'-(1*H*-indole-3yl)-2-oxospiro[indoline-3,4'-pyran]-3'-carboxylate.

hineylide generated from isatin and sarcosine with the dipolarphile 3-(1*H*-indole-3-yl)-3-oxo-2-(2-oxoindolin-3-ylide-ne) propanenitrile and also spiro compound of acenapht-henequinone obtained by the same optimized reaction condition [7]. The synthesized compounds were evaluated for their antimicrobial activity and all the compounds showed significant activity. Non-isothermal decomposition kinetics of chitosan [8], chitin [9], cephalosporins [10], procaine and benzocaine [11], theobromine [12], spiro-oxindole derivatives [13-15], parthenium hysterophorus [16], nitroimidazoles [17] and ferrocene [18] were studied in detail and appropriate kinetic models were proposed.

In this manuscript, we report the synthesis and charac-terization of ethyl-2'-amino-5'-cyano-6'-(1*H*-indole-3yl)-2-oxospiro[indoline-3,4'-pyran]-3'-carboxylate (EACIOIPC) (Figure 1) [19] and its thermal decomposition under non-isothermal condition in dynamic nitrogen atmosphere. The thermal decomposition of EACIOIPC spiro-derivative com-pound was studied by using TG/DTG and DTA methods. To our knowledge, the thermodynamic and kinetic data of the thermal decomposition of EACIOIPC have not been reported. In this report, the kinetic and thermodynamic parameters were computed by using model-fitting and model free-methods.

2. Experimental

2.1. Materials

Isatin, cyanoethylacetate, 3-cyanoacetyl indole and DMSO-d_6 were purchased from Aldrich Chemicals. Acetic anhydride and other reagents were procured from SD Fine Chemicals and were used as received.

2.2. Instrumentations

Elemental analyses were performed at Central Leather Research Institute (CLRI), Chennai, India. IR measurements were done as KBr pellets for solids using Perkin Elmer Spectrometer RXI FT-IR. The ^{1}H and ^{13}C NMR spectra were recorded in DMSO-d_6 using TMS as internal standard with JEOL ECA-500MHz NMR spectrometer. The mass spectrum was recorded using electrospray ionization method with Thermo Finnigan mass spectrometer. Melting points were determined in capillary tubes and are uncorrected. Analytical TLC was performed on pre-coated plastic sheets of silica gel G/UV-254 of 0.2 mm thickness. The simultaneous TGA curves were obtained with the thermal analysis system model Perkin Elmer TAC7/DX (Thermal Analysis Controller TAC-7). The TG analyses of EACIOIPC were carried out under dynamic nitrogen atmosphere (100 mL/min) in an iron pan with the sample at the heating rates of 10, 15, 20 and 30 K/min from 30 to 850 °C. TGA were recorded at Indian Institute of Technology, Chennai, India. The kinetic parameters E_a and A were calculated using Microsoft Excel Software. The sample temperature, controlled by thermocouple, did not exhibit any systematic deviation from the preset linear temperature program.

2.3. Synthesis of ethyl-2'-amino-5'-cyano-6'-(1H-indole-3yl)-2-oxospiro[indoline-3,4'-pyran]-3'-carboxylate

To a stirred solution of isatin (0.294 g, 2 mmol), cyano ethylacetate (0.122 g, 2 mmol), and 3-cyanoacetyl indole (0.368 g, 2 mmol) in methanol (20 mL), triethyl amine (20 mol %) was added and stirring was continued. On completion, the reaction mixture was poured into crushed ice and the precipitate formed was filtered, dried and purified by column chromatography to afford the pure product. The isolated product was further purified by recrystallization in ethanol and the yield of the product was 90 %. Color: Pale brown solid. Yield: 78%. M.p.: 223-225 °C. R_f: 0.25 (40% AcOEt/Petroleum ether). FT-IR (KBr, ν, cm^{-1}): 3367 (NH$_2$), 3253 (NH), 2985 (C$_2$H$_5$), 2208 (C≡N), 1630 (C=O), 1623 (COO$^-$), 1518 (C$_6$H$_5$), 1142 (C-O-C). ^{1}H NMR (500 MHz, DMSO-d_6, δ, ppm): 0.72 (t, *J* = 6.9 Hz, 3H, CH$_3$), 3.28 (s, 2H, NH$_2$), 3.70-3.73 (m, 2H, CH$_2$), 6.82-6.84 (m, 1H, Ar-H), 6.94 (t, *J* = 7.65 Hz, 1H, Ar-H), 7.12-7.22 (m, 3H, Ar-H), 7.49 (d, *J* = 8.4 Hz, 1H, Ar-H), 7.95-8.09 (m, 3H, Ar-H), 10.54 (brs, 1H,NH), 12.00 (brs, 1H, NH). ^{13}C NMR (125 MHz, DMSO-d_6, δ, ppm): 14.2, 46.3, 61.7, 79.8, 80.4, 102.0, 111.1, 117.3, 119.0, 120.1, 122.1, 124.9, 126.1, 127.8, 129.9, 130.8, 135.5, 141.2, 159.9, 162.2, 167.2, 168.2. MS (EI, *m/z*): 427.13 [M$^+$+H$^+$].

3. Theoretical background

3.1. Model fitting method

There are numerous non-isothermal model-fitting methods, and the most popular one is the Coats and Redfern method [20]. This method has been successfully used for studying the kinetics of dehydration and decomposition of different solid substances [21]. The kinetic parameters can be derived from the modified Coats and Redfern Equation (1),

$$\ln\left[\frac{g(\alpha)}{T^2}\right] = \ln\left(\frac{AR}{\beta E_a}\left[1 - \left(\frac{2RT^*}{E_a}\right)\right]\right) - \frac{E_a}{R \times T} \tag{1}$$

where g(α) is an integral form of the conversion function (α), the expression of which depends on the kinetic model of the occurring reaction. If the correct g(α) function is used, a plot of ln[g(α)/T^2] against 1/T should give a straight line from which the values of the activation energy, E_a and the pre-exponential factor, *A* can be calculated.

3.2. Model free methods

Friedman method [22] is a differential method and is one of the first used iso-conversional methods. This model according to logarithmic form of Equation (3).

$$\frac{d\alpha}{dt} = A\exp\left(\frac{-E_a}{RT}\right)f(\alpha) \tag{2}$$

gives

$$\ln\left[\beta\frac{d\alpha}{dT}\right] = \ln[A_\alpha f(\alpha)] - \frac{E_{a,\alpha}}{RT_\alpha} \quad (3)$$

The plots of $\ln(\beta.d\alpha/dT)$ *vs* $1/T$ (Equation(3)), at each α value were drawn and from the slope of the plots, we can calculate E_a values.

The isoconversional integral method suggested independently by Flynn and Wall [23] and Ozawa [24], and is based on the Equation (4),

$$\ln\beta = \ln\left[\frac{0.0048AE_a}{g(\alpha)R}\right] - 1.0516\left(\frac{E_a}{RT}\right) \quad (4)$$

and Kissinger-Akahira-Sunose (KAS) method [25,26], Equation (5) is used.

$$\ln(\beta/T^2) = \ln\left[\frac{AE_a}{g(\alpha)R}\right] - \frac{E_a}{RT} \quad (5)$$

The plots of $\ln(\beta.d\alpha/dT)$ *vs* $1/T$ (Equation(3)), $\ln\beta$ *vs* $1/T$ (Equation (4)) and $\ln(\beta/T^2)$ *vs* $1/T$ (Equation (5)) has been shown to give the values of apparent activation energies for the decomposition of EACIOIPC at different values of α. According to these equations, the reaction mechanism and shape of $g(\alpha)$ function do not affect the values of the activation energies of the decomposition stages.

3.3. Invariant kinetic parameters method

The invariant kinetic parameters are obtained by the method of Lesnikovich and Levchik [27]. The straight lines obtained for the plots of $\ln A_\beta$ *vs* E_β for several constant heating rates should intersect at a point [28] which corresponds to the true values of activation energy and pre-exponential factor and they are named invariant kinetic parameters (E_{inv}, A_{inv}) which are evaluated using the super correlation relation Equation (6),

$$a_\beta = \ln A_{inv} - b_\beta \times E_{inv} \quad (6)$$

Plot of a_β *vs* b_β gives a straight line, the values of E_{inv} and $\ln A_{inv}$ are calculated from the slope and intercept of the plot, respectively.

3.4. Thermodynamic parameters

The kinetic parameters, energy of activation (E_a) and pre-exponential factor (A) are obtained from Kissinger single point kinetic method which uses the Equation (7),

$$\ln\left(\frac{\beta}{T_m^2}\right) = -\frac{E_a}{RT_m} + \ln\left(\frac{AR}{E_a}\right) \quad (7)$$

where T_m is temperature that corresponds to the maximum of $d\alpha/dT$. This model-free kinetic method can be applied with a reasonable approximation without being limited to n-order kinetics [29], providing a single E_a value for each reaction step. For this reason, it is often defined as a Kissinger single point method. The reaction proceeds under conditions where thermal equilibrium is always maintained, then a plot of $\ln\left(\frac{\beta}{T_m^2}\right)$ *vs* $\frac{1}{T_m}$ gives a straight line with a slope equal to $-E_a/R$.

Based on the values of activation energy and pre-exponential factor for the decomposition stage, the values of $\Delta S^{\neq}$, $\Delta H^{\neq}$ and $\Delta G^{\neq}$ for the formation of activated complex from the reactant were calculated based on the following Equations (8-10) [30-32],

$$\Delta S^{\neq} = R\ln\frac{Ah}{e\chi k_B T_p} \quad (8)$$

Since

$$\Delta H^{\neq} = E_a - RT_p \quad (9)$$

$$\Delta G^{\neq} = \Delta H^{\neq} - T_p\Delta S^{\neq} \quad (10)$$

4. Results and discussion

4.1. Non-isothermal TGA

The thermograms of pure EACIOIPC recorded in a dynamic nitrogen atmosphere at different heating rates of 10, 15, 20 and 30 K/min are presented in Figure 2. They show two distinct endothermic peaks due to melting and decomposition. The thermal decomposition process of EACIOIPC in three stages is observed from the TGA curves. The decomposition process for first stage starts at 483 K and ends at 563 K with the mass loss of 47.0%. The second stage decomposition starts at 653 K and ends at 773 K with the mass loss of 10.09%. The third stage of decomposition starts at 773 K and ends at 1113 K with the mass loss of 17.38%.

4.2. Model-free analysis

The non-isothermal decomposition kinetics of EACIOIPC is first analyzed by model-free methods viz., Friedman, Kissinger- Akahira-Sunose and Flynn-Wall-Ozawa. Tables 1-3 show the variation of apparent activation energy E_a, as a function of extent of conversion α, for the decomposition of EACIOIPC. E_a value increases slightly in the conversion range of $0.12 \leq \alpha \leq 0.98$ for all the stages. It was pointed out [33] that when E_a changes with α, the Friedman and KAS iso-conversional methods lead to close values of E_a for all the stages. The applied iso-conversional methods do not suggest a direct way for evaluating either the pre-exponential factor (A) or the analytical form of the reaction model f(α), for the investigated decomposition process of EACIOIPC.

For the first stage decomposition of EACIOIPC, the values of energy of activation corresponding to the different values of α for the decomposition process obtained by Friedman, KAS and FWO methods are listed in T (Figure 3). It is seen that E_a value depends upon the extent of conversion α. The average value of E_a is 245.59±0.85 kJ/mol (KAS method). From Figure 3, it is evident that the values of activation energy obtained by Friedman and FWO methods (245.01±0.16 kJ/mol, Friedman; 240.94±0.43 kJ/mol, FWO) are slightly lesser than that of KAS method.

For stage II the variation of E_a with α for the decomposition is shown in Figure 4. The average value of E_a is 283.21±0.16 kJ/mol (Friedman method). From Table 2, it is evident that the Friedman method activation energy is higher than the values of activation energy obtained by KAS (E_a = 275.58±0.28 kJ/mol) and FWO (E_a = 270.96±0.08 kJ/mol) methods.

For stage III, the values of apparent activation energies obtained by Friedman and KAS methods are higher than that of FWO method. The average values of E_a in the range $0.12 \leq \alpha \leq 0.98$ were 629.45±0.60 kJ/mol (Friedman), 620.30±0.51 kJ/mol (KAS), and 604.26±0.55 kJ/mol (FWO), (Figure 5). Form Table 3, it is evident that the Friedman method and KAS methods gave higher values of activation energy than the FWO method.

From the average values of E_a for each stage, the rate of decomposition is found to depend upon the nature of the intermediate formed during the decomposition. The third stage is slower than the other stages of decomposition.
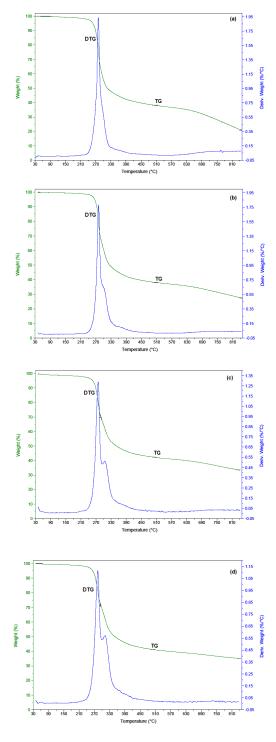
Figure 2. TG and DTG curves of EACIOIPC at (a) 10, (b) 15, (c) 20 and (d) 30 K/min heating rates in oxygen atmosphere.

The higher value of activation energy for Stage III than the other stages indicates that the intermediate compounds are thermally more stable and hence the decomposition process is slow.

4.3. Model-fitting analysis

After carrying out model-free analysis, model-fitting can be done in the conversion region where apparent activation energy is approximately constant where a single model may fit. The non-isothermal kinetic data of EACIOIPC at $0.12 \leq \alpha \leq$ 0.98 where model-free analysis indicates approximately constant activation energy, were then fitted in to each of the 15 models listed in Tables 1 for Stages 1, 2, and 3, respectively.

As shown in Tables 2-4, for the applied method, Arrhenius parameters (E_a, ln A) for decomposition process, exhibit strong dependence on the reaction model chosen.

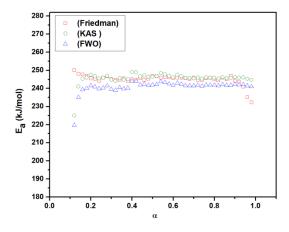### 4.4. Invariant kinetics parameters analysis

Criado and Morales [34] reported that almost any $\alpha = \alpha(T)$ or $(d\alpha/dt)$ (T) experimental curve may be correctly described by several conversion functions.

Table 1. Algebraic expressions of f(α) and g(α) for the reaction models considered in the present work.

S. No.	Symbol	Reaction Model	Differential form [a] $f(\alpha) = (1/k)(d\alpha/dt)$	Integral form [a] $g(\alpha) = kt$
Nucleation models				
1	P2	Power law	$3\alpha^{(2/3)}$	$\alpha^{(1/3)}$
2	P3	Power law	$2\alpha^{(1/2)}$	$\alpha^{(1/2)}$
3	P4	Power law	$2/3\alpha^{-1/2}$	$\alpha^{(3/2)}$
Reaction-order models				
4	F1	First-order (Mampel)	$(1-\alpha)$	$-\ln(1-\alpha)$
5	F2	Second-order	$(1-\alpha)^2$	$(1-\alpha)^{-1}-1$
6	F3	Third-order	$(1-\alpha)^3$	$0.5[(1-\alpha)^{-2}-1]$
Diffusion models				
7	D1	1-D Diffusion	$1/2\alpha^{-1}$	α^2
8	D2	2-D Diffusion	$[-\ln(1-\alpha)]^{-1}$	$[(1-\alpha)\ln(1-\alpha)]+\alpha$
9	D3	3-D Diffusion-Jandereqn.	$2(1-\alpha)^{2/3}[1-(1-\alpha)^{1/3}]^{-1}$	$[1-(1-\alpha)^{1/3}]^2$
10	D4	Ginstling-Brounshtein	$3/2[(1-\alpha)^{-1/3}-1]$	$(1-2\alpha/3)-(1-\alpha)^{2/3}$
11	A2	Avrami-Erofe'ev	$2(1-\alpha)[-\ln(1-\alpha)]^{1/2}$	$[-\ln(1-\alpha)]^{1/2}$
12	A3	Avrami-Erofe'ev	$3(1-\alpha)[-\ln(1-\alpha)]^{2/3}$	$[-\ln(1-\alpha)]^{1/3}$
13	A4	Avrami-Erofe'ev	$4(1-\alpha)[-\ln(1-\alpha)]^{3/4}$	$[-\ln(1-\alpha)]^{1/4}$
Geometrical contraction models				
14	R2	Phase-boundary controlled reaction (contracting volume i.e., bidimensional shape)	$2(1-\alpha)^{1/2}$	$[1-(1-\alpha)^{1/2}]$
15	R3	Phase-boundary controlled reaction (contracting volume i.e., tridimensional shape)	$3(1-\alpha)^{2/3}$	$[1-(1-\alpha)^{1/3}]$

Table 2. Arrhenius parameters for non-isothermal decomposition of compound EACIOIPC (Stage I) at various heating heats.

Kinetic model	β = 10 K/min			β = 15 K/min			β = 20 K/min			β = 30 K/min		
	E_a (kJ/mol)	$\ln A$	r	E_a (kJ/mol)	$\ln A$	r	E_a (kJ/mol)	$\ln A$	r	E_a (kJ/mol)	$\ln A$	r
P2	2.71	-3.86	-0.891	2.71	-3.47	-0.893	2.62	-3.25	-0.887	2.60	-2.87	-0.886
P3	-0.71	-	0.648	-0.72	-	0.658	-0.79	-	0.692	-0.82	-	0.707
P4	-2.41	-	0.973	-	-	0.974	-2.49	-	0.976	-2.53	-	0.977
F1	22.64	3.46	-0.934	22.71	3.85	-0.935	22.53	4.04	-0.934	22.57	4.41	-0.934
F2	36.02	7.87	-0.895	36.14	8.27	-0.896	35.89	8.42	-0.895	35.97	8.77	-0.895
F3	52.58	13.10	-0.867	52.77	13.50	-0.868	52.43	13.61	-0.867	52.57	13.95	-0.867
D1	40.86	14.87	-0.987	40.98	15.27	-0.987	40.78	15.44	-0.987	40.90	15.81	-0.987
D2	38.79	6.59	-0.974	38.90	6.99	-0.975	38.65	7.14	-0.974	38.74	7.49	-0.974
D3	45.56	7.27	-0.962	45.70	7.67	-0.962	45.41	7.80	-0.962	45.52	8.14	-0.962
D4	41.02	5.82	-0.970	41.14	6.21	-0.971	40.88	6.35	-0.970	40.98	6.70	-0.970
A2	7.56	-1.38	-0.874	7.57	-0.99	-0.876	7.46	-0.76	-0.873	7.46	-0.39	-0.873
A3	2.52	-3.73	-0.680	2.52	-3.34	-0.682	2.43	-3.12	-0.670	2.41	-2.75	-0.667
A4	0.01	-9.79	-0.006	0.00	-10.30	-0.002	-0.07	-	0.036	-0.10	-	0.050
R2	17.35	0.92	-0.955	17.39	1.31	-0.956	17.24	1.52	-0.955	17.27	1.88	-0.955
R3	15.85	0.65	-0.961	15.89	1.05	-0.962	15.74	1.26	-0.962	15.76	1.63	-0.961

Figure 3. E_a versus α plot for the decomposition of EACIOIPC under non-isothermal condition (Stage I).

The use of an integral or differential model-fitting method leads to different values of the activation parameters. Although obtained with high accuracy the values change with different heating rates and among conversion functions.

Lesnikovich and Levchik [27,28] suggested that correlating these values by the apparent compensation effect, $\ln A = a_\beta + b_\beta E_a$, one obtains the compensation effect parameters a_β and b_β, which strongly depend on the heating rates (β) as well as on the considered set of conversion functions. The straight lines of $\ln A$ vs E_a for four constant heating rates should intersect at a point (iso-parametric point) which corresponds

to the true values of the activation energy and pre-exponential factor. These were named as invariant kinetic parameters.
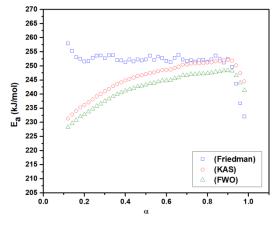
The invariant kinetic parameters method was applied to the data calculated for the heating rates of 10, 15, 20 and 30 K/min. The evaluation of the kinetic parameters was performed using Coats-Redfern method. For these kinetic models in the range $0.12 \le \alpha \le 0.98$ for EACIOIPC for all the stages, the straight lines corresponding to Coats-Redfern method is characterized by correlation coefficient values close to unity.

Table 3. Arrhenius parameters for non-isothermal decomposition of compound EACIOIPC (Stage II) at various heating rates.

Kinetic model	β = 10 K/min			β = 15 K/min			β = 20 K/min			β = 30 K/min		
	E_a (kJ/mol)	ln A	r	E_a (kJ/mol)	ln A	r	E_a (kJ/mol)	ln A	r	E_a (kJ/mol)	ln A	r
P2	44.73	7.51	-0.883	46.67	8.32	-0.893	46.59	8.53	-0.894	45.77	8.65	-0.881
P3	26.67	3.23	-0.860	27.95	3.92	-0.872	27.88	4.15	-0.872	27.31	4.35	-0.857
P4	17.69	0.94	-0.830	18.64	1.58	-0.845	18.57	1.82	-0.845	18.13	2.06	-0.827
F1	162.69	34.24	-0.957	168.54	35.76	-0.961	168.35	35.81	-0.962	166.51	35.52	-0.955
F2	255.26	55.11	-0.984	263.80	57.11	-0.987	263.50	57.03	-0.987	261.40	56.53	-0.983
F3	372.08	81.20	-0.994	383.95	83.79	-0.995	383.51	83.56	-0.996	381.15	82.81	-0.993
D1	220.48	53.41	-0.915	228.60	55.37	-0.921	228.47	55.37	-0.922	225.41	54.74	-0.913
D2	241.04	49.93	-0.926	249.99	52.04	-0.933	249.77	52.00	-0.933	246.54	51.28	-0.925
D3	285.91	58.53	-0.945	296.21	60.88	-0.950	295.92	60.77	-0.951	292.52	59.94	-0.943
D4	255.78	51.75	-0.933	265.18	53.94	-0.939	264.93	53.87	-0.940	261.65	53.12	-0.932
A2	76.67	15.13	-0.951	79.57	16.10	-0.957	79.45	16.27	-0.957	78.50	16.31	-0.950
A3	47.93	8.52	-0.945	49.86	9.32	-0.951	49.76	9.52	-0.952	49.10	9.68	-0.943
A4	33.65	5.12	-0.938	35.09	5.83	-0.945	35.00	6.05	-0.946	34.49	6.26	-0.936
R2	127.25	25.46	-0.933	132.05	26.79	-0.939	131.90	26.89	-0.939	130.20	26.69	-0.931
R3	117.42	23.48	-0.923	121.92	24.76	-0.930	121.79	24.87	-0.931	120.13	24.70	-0.921

Table 4. Arrhenius parameters for non-isothermal decomposition of compound EACIOIPC (Stage III) at various heating rates.

Kinetic model	β = 10 K/min			β = 15 K/min			β = 20 K/min			β = 30 K/min		
	E_a (kJ/mol)	ln A	r	E_a (kJ/mol)	ln A	r	E_a (kJ/mol)	ln A	r	E_a (kJ/mol)	ln A	r
P2	-3.47	-	0.941	-3.55	-	0.942	-3.58	-	0.943	-3.66	-	0.947
P3	-7.07	-	0.995	-7.14	-	0.994	-7.17	-	0.994	-7.25	-	0.995
P4	-8.86	-	0.998	-8.93	-	0.998	-8.96	-	0.998	-9.04	-	0.998
F1	17.51	-1.59	-0.897	17.40	-1.23	-0.896	17.39	-0.96	-0.895	17.32	-0.59	-0.895
F2	31.62	1.40	-0.865	31.48	1.75	-0.864	31.48	2.02	-0.863	31.42	2.38	-0.864
F3	49.09	4.77	-0.843	48.92	5.12	-0.843	48.92	5.38	-0.842	48.89	5.73	-0.843
D1	42.05	9.83	-0.985	41.96	10.20	-0.985	42.00	10.47	-0.985	42.00	10.84	-0.985
D2	34.47	-0.20	-0.966	34.33	0.16	-0.966	34.34	0.43	-0.966	34.27	0.79	-0.966
D3	41.61	-0.27	-0.953	41.46	0.08	-0.952	41.47	0.35	-0.952	41.41	0.70	-0.952
D4	36.83	-1.22	-0.961	36.68	-0.87	-0.961	36.69	-0.60	-0.961	36.63	-0.24	-0.961
A2	1.64	-5.95	-0.380	1.55	-5.62	-0.363	1.52	-5.36	-0.356	1.45	-5.03	-0.344
A3	-3.67	-	0.833	-3.74	-	0.838	-3.77	-	0.839	-3.85	-	0.847
A4	-6.30	-	0.966	-6.38	-	0.967	-6.41	-	0.967	-6.48	-	0.969
R2	11.93	-3.64	-0.914	11.82	-3.27	-0.912	11.81	-3.00	-0.912	11.74	-2.63	-0.912
R3	10.35	-3.78	-0.918	10.24	-3.41	-0.917	10.23	-3.14	-0.916	10.16	-2.77	-0.917

Figure 4. E_a versus α plot for the decomposition of EACIOIPC under non-isothermal condition (Stage II).
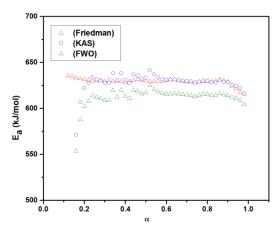

Figure 5. E_a versus α plot for the decomposition of EACIOIPC under non-isothermal condition (Stage III).
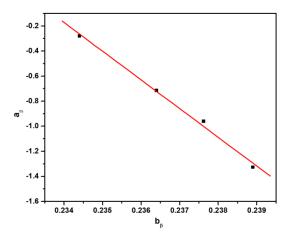
Figure 6. Super correlation (compensation effect parameters) plot for the best combination of kinetic models (Stage I).
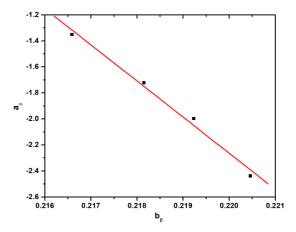

Figure 7. Super correlation (compensation effect parameters) plot for the best combination of kinetic models (Stage II).
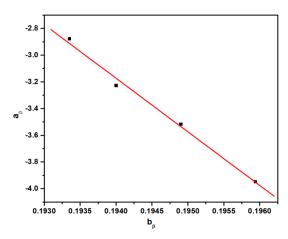

Figure 8. Super correlation (compensation effect parameters) plot for the best combination of kinetic models (Stage III).

For several groups of apparent activation parameters, obtained by different kinetic models, we tried to establish the best correlation ($r \to 1$), a better resolution in determining the invariant kinetics parameters and the closet value to the mean iso-conversional activation energies.

For Stage I for AKM–{P2;A3}, the plot of ln A vs E_a has the highest correlation coefficient and is a straight line (Figure 6). The invariant kinetic parameters, E_{inv} = 250.68±0.72 kJ/mol for AKM and ln A_{inv} = 80.56 are obtained with r = 0.995 (Figure 6). For these groups, the invariant activation energy is high

250.68 kJ/mol compared to Friedman, KAS and FWO methods (245.59±0.85, 245.01±0.16, 240.94±0.43 kJ/mol, respectively).

For Stage II, a better resolution in determining the invariant kinetic parameters, and the correlation coefficients (Figure 7) show a good agreement of all kinetic models. The efficiency of IKP method is strongly revealed by AKM-{F2;D1;D4} (Figure 7) and even by AKM (all kinetic models) which comprises all the best-fitting function that makes it a more powerful method. The invariant activation energy is 283.21 kJ/mol, which is close to Friedman method.
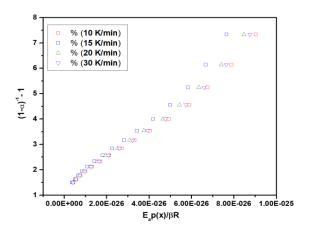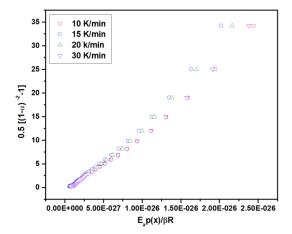
Figure 9. Determination of *A* value by plotting $(1-\alpha)^{-1}-1$ against $E_a \times p(x)/\beta \times R$ for the decomposition of EACIOIPC at different heating rates (β) (Stage I).
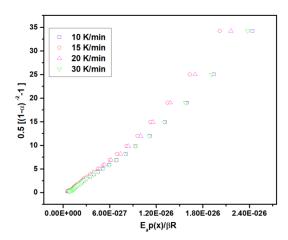

Figure 10. Determination of *A* value by plotting $0.5[(1-\alpha)^{-2}-1]$ against $E_a \times p(x)/\beta \times R$ for the decomposition of EACIOIPC at different heating rates (β) (Stage II).

Figure 11. Determination of *A* value by plotting $0.5 \times [(1-\alpha)^{-2}-1]$ against $E_a \times p(x)/\beta \times R$ for the decomposition of EACIOIPC at different heating rates (β) (Stage III).

The invariant kinetic parameters are E_{inv} = 277.38 kJ/mol and ln A_{inv} = 58.76 obtained with r = 0.994.

For third stage of AKM-{A2;R2}, the plot of ln A versus E_a has the highest correlation coefficient (r = 0.883) (Figure 8). Depending upon the choice of kinetic models, the compensation effect parameters are obtained with different accuracies, their values and the derived invariant activation parameters varying substantially. For AKM-{A2;R2}, the invariant kinetic parameters are 673.73 kJ/mol and ln A_{inv} = 130.68 obtained with r = 0.883. For these groups, the invariant activation energy is high in comparison with Friedman, KAS

and FWO methods (629.45±0.60 kJ/mol, Friedman; 620.30±0.51 kJ/mol, KAS; 604.26±0.55 kJ/mol, FWO).

4.5. Determination of kinetic models

The most suitable kinetic model for the decomposition process of EACIOIPC is F2. By introducing the derived reaction model g(α) =$(1-\alpha)^{-1}-1$, the following equation is obtained.

$$\left(1-\alpha\right)^{-1}-1 = \frac{AE_a}{\beta R}p(x) \tag{11}$$

Table 5. Values of kinetic and thermodynamic parameters for the thermal decomposition of EACIOIPC in nitrogen atmosphere.

Parameter	Stage I	Stage II	Stage III
E_a (kJ/mol)	687.51	223.97	323.49
ln A	17.82	48.80	44.17
$\Delta G^{\neq}$ (kJ/mol)	113.91	137.73	224.45
$\Delta H^{\neq}$ (kJ/mol)	65.00	219.36	316.23
$\Delta S^{\neq}$ (J/K.mol)	-108.49	147.41	105.10
r	0.991	0.988	0.993

The plots of $(1-\alpha)^{-1}-1$ against $E_a \times p(x)/\beta \times R$ at the different heating rates are shown in Figure 9. The activation energy for Stage I, E_a = 245.59 kJ/mol and the frequency factor was found to be 9.699×10^{34} min^{-1} (ln A = 80.56). The obtained value of ln A is in good agreement with values obtained by Friedman iso-conversional intercept.

The most suitable kinetic model is F3 for stages II and III as confirmed by introducing the derived reaction model $g(\alpha)$ = 0.5 $[(1-\alpha)^{-2} -1]$, when the following equation is obtained [30].

$$0.5 \times \left[(1-\alpha)^{-2} - 1 \right] = \frac{AE_a}{\beta R} p(x) \qquad (12)$$

The plots of $0.5 \times [(1-\alpha)^{-2}-1]$ against $E_a \times p(x)/\beta \times R$ at the different heating rates are shown in Figures 10 and 11. The activation energy E_a = 283.21 kJ/mol and frequency factor for Stage III is 3.304×10^{25} min^{-1} (ln A = 58.76) and the activation energy E_a = 629.45 kJ/mol and the frequency factor for Stage IV is 5.670×10^{56} min^{-1} (ln A = 130.68) as determined by IKP method. Venkatesan *et al.,* non-isothermal decomposition of 4-((4-fluoro-3-phenoxy-benzylidene)amino) benzene sulfon-amide under oxygen atmosphere [35] decomposition kinetics model F2, and Manikandan *et al.,* 1,5-*bis*(4-hydroxy-3-methoxy phenyl)pentan-1,4-diene-3-one compound was decomposed under R2 model [36].

4.6. Thermodynamic parameters

From the DTG curves, the peak temperatures of EACIOIPC are 450.82, 553.81 and 873.21 K. These peak temperatures are used to evaluate single point kinetic parameters [25]. The obtained values are 687.51, 223.97, 323.49 kJ/mol for Stages I, II and III, respectively. The thermodynamic parameters, $\Delta S^{\neq}$, $\Delta H^{\neq}$ and $\Delta G^{\neq}$ were calculated at the peak temperature T_m in the DTG curves for the corresponding stage [37,38] since the temperature characterizes the higher rate of decomposition.

As can be seen from Table 5, the value of $\Delta S^{\neq}$ for the decomposition is positive for Stages II and III. It means that the corresponding activated complexes were with lesser degrees of arrangement than the initial state, whereas for the first stage the transition state was more ordered than the initial stage. The positive values of $\Delta H^{\neq}$ and $\Delta G^{\neq}$ show that they are connected with absorption of heat and are non-spontaneous processes [39]. The obtained E_a values coincide with invariant parameters.

5. Conclusion

The compound chosen for the study decomposed in three stages. Activation energies of three stages of obtained compound could be determined from a model-free analysis and model-fitting analysis of TGA data. Since, the activation energy values varied with conversion level, the activation energy values were used to interpret decomposition models for each stages followed by different kinetic models namely F2 for first stage and F3 for second and third stages. The rate of decomposition of third stage is slow due to high energy of activation when compared to Stages I and II. The positive free energy values indicated that the decomposition of studied compound is non-spontaneous process.

Disclosure statement DS

Conflict of interests: The authors declare that they have no conflict of interest.
Author contributions: All authors contributed equally to this work.
Ethical approval: All ethical guidelines have been adhered.
Sample availability: Samples of the compounds are available from the author.

ORCID

Ganesan Nalini
http://orcid.org/0000-0001-6072-1713
Natesan Jayachandramani
http://orcid.org/0000-0002-7087-9722
Radhakrishnan Suresh
http://orcid.org/0000-0002-9340-317X
Prakasam Thirumurugan
http://orcid.org/0000-0003-3450-6328
Venugopal Thanikachalam
http://orcid.org/0000-0003-1076-6272
Govindasamy Manikandan
http://orcid.org/0000-0003-2732-4366
Dharmalingam Sankari
http://orcid.org/0000-0002-3553-9626

References

[1]. Bhaskar, G.; Arun, Y.; Balachandran, C.; Saikumar, C.; Perumal, P. T. *Eur. J. Med. Chem.* **2012**, *51*, 79-91.
[2]. Gribble, G. W. *J. Chem. Soc. Perkin Trans. I* **2000**, 1045-1075.
[3]. Zhu, S. L.; Ji, S. L.; Su, X. M.; Sun, C.; Liu, Y. *Tetrahedron Lett.* **2008**, *49,* 1777-1781.
[4]. Farghaly, A. M.; Habib, N. S.; Khalil, M. A.; El-Sayed, O. A. *Alexandria. J. Pharm. Sci.* **1989**, *3,* 84-86.
[5]. Yu, B.; Yu, D. Q.; Liu, H. M. *Eur. J. Med. Chem.* **2015**, *97*, 673-698.
[6]. Fuchao, Y.; Huang, R.; Hangchen, N.; Juan, F.; Shengjiao, Y.; Lin, L. *Green. Chem.* **2013**, *15,* 453-462.
[7]. Arun, Y.; Bhaskar, G.; Balachandran, C.; Ignacimuthu, S.; Perumal, P. T. *Bioorg. Med. Chem. Lett.* **2013**, *23*, 1839-1845.
[8]. Georgieva, V.; Zvezdova, D.; Vlaev, L. *Chem. Cent. J.* **2012**, *6*, 81, 1-10
[9]. Georgieva, V.; Zvezdova, D.; Vlaev, L. *J. Therm. Anal. Calorim.* **2013**, *111*, 763-771.
[10]. Fulias, A.; Vlase, G.; Vlase, T.; Soica, C.; Heghes, A.; Craina, M.; Ledeti, I. *Chem. Cent. J.* **2013**, *7*, 70, 1-8.
[11]. Fulias, A.; Vlase, G.; Grigorie, C.; Ledeti, I.; Albu, P.; Bilanin, M.; Vlase, T. *J. Therm. Anal. Calorim.* **2013**, *113,* 265-271.
[12]. Kamel, T. L. *Eur. J. Chem.* **2015**, *6(2),* 199-203.
[13]. Nalini, G.; Jayachandramani, N.; Thanikachalam, V.; Jayabharathi, J.; Manikandan, G.; Suresh, R. *Can. Chem. Trans.* **2016**, *4,* 62-72.
[14]. Nalini, G.; Jayachandramani, N.; Suresh, R.; Thanikachalam, V.; Manikandan, G. *Eur. J. Chem.* **2016**, *7(3),* 380-386.
[15]. Nalini, G.; Jayachandramani, N.; Suresh, R.; Thirumurugan, P.; Thanikachalam, V.; Manikandan, G. *Int. J. Adv. Chem. Sci. App.* **2016**, *3(4),* 25-38.
[16]. Alok, D.; Suraj, B. S.; Muammel, M. H.; Rekha, R. *Environ. Clim. Technol.* **2018**, *22,* 5-21.

[17]. Venkatesh, M.; Ravi, P.; Surya, P. T. *J. Phys. Chem. A* **2013**, *117*, 10162-10169.
[18]. Ashis, B.; Amlan, R.; Debasis, R.; Madhusudan, R. *J. Exp. Phys.* **2014**, Article ID: 513268.
[19]. Nandakumar, A.; Thirumurugan, P.; Perumal, P. T.; Vembu, P.; Ponnuswamy, N. M.; Ramesh, P. *Bioorg. Med. Chem. Lett.* **2010**, *20*, 4252-4258.
[20]. Coats, A. W.; Redfern, J. P. *Nature (London)* **1968**, *201,* 68-69.
[21]. Wendlandt, W. W. Thermal Methods of Analysis, John Wiley and Sons Inc., New York, 1974.
[22]. Friedman, H. L. *Polym. Sci.* **1963**, *6*, 183-195.
[23]. Flynn, J. H.; Wall, L. A. *J. Res. Natl. Bur. Stand.* **1966**, *70,* 487-523.
[24]. Ozawa, T. *Bull. Chem. Soc. Jpn.* **1965**, *38*, 1881-1886.
[25]. Kissinger, H. E. *Anal. Chem.* **1957**, *29*, 1702-1706.
[26]. Akahira, T.; Sunose, T. *Res. Rep. CHIBA Inst. Technol.* **1971**, *16,* 22-31.
[27]. Lesnikovich, A. I.; Levchik, S. V. *J. Therm. Anal.* **1985**, *30,* 237-262.
[28]. Lesnikovich, A. I.; Levchik, S. V. J. *Therm. Anal.* **1983**, *27,* 89-94.

[29]. Malek, J. A. *Thermochim. Acta* **1989**, *136,* 337-346.
[30]. Malek, J. *Thermochim. Acta* **1992**, *200,* 257-269.
[31]. Cordes, F. H. *J. Phys. Chem.* **1968**, *72,* 2185-2189.
[32]. Bamford, C. H.; Tipper, C. F. H. *Comprehensive chemical kinetics, Reactions in the Solid State* **1980**, *22,* 1-340.
[33]. Pratap, A.; Rao, T. L. S.; Dhaurandhar, H. D. *J. Therm. Anal. Calorim.* **2007**, *89,* 399-405.
[34]. Criado, J. M.; Morales, J. *Thermochim. Acta* **1976***, 16,* 382-387
[35]. Venkatesan, J.; Sekar, M.; Thanikachalam, V.; Manikandan, G. *Chemical Data Collections,* **2017**, *9(10)*, 67-79.
[36]. Manikandan, G.; Rajarajan, G.; Jayabharathi, J.; Thanikachalam, V. *Arab. J. Chem.* **2011**, *9,* 570-575.
[37]. Ma, H. X.; Yan, B.; Li, Z. N.; Song, J. R.; Hu, R. Z. *J. Therm. Anal. Calorim.* **2007**, *95,* 437-444.
[38]. Boonchom, B. *J. Therm. Anal. Calorim.* **2010**, *31,* 416-429.
[39]. Criado, J. M.; Perez-Maqueda, L. A.; Sanchez-Jimenez, P. E. *J. Therm. Anal. Calorim.* **2005**, *82,* 671-675.